Journal of Marine Systems 166 (2017) 132–143

Contents lists available at ScienceDirect

Journal of Marine Systems

journal homepage: www.elsevier.com/locate/jmarsys

Effects of physical constraints on the lability of POM during summer in the Ross Sea

Cristina Misic [a,*], Anabella Covazzi Harriague [a], Olga Mangoni [b], Giuseppe Aulicino [c,d], Pasquale Castagno [c], Yuri Cotroneo [c]

[a] Dipartimento di Scienze della Terra, dell'Ambiente e della Vita, University of Genova, C.so Europa 26, 16132 Genova, Italy
[b] Dipartimento di Biologia, University of Napoli Federico II, Via Mezzocannone, 8, 80134 Napoli, Italy
[c] Dipartimento di Scienze e Tecnologie, University of Napoli Parthenope, Centro Direzionale di Napoli IS. C4, 80143 Napoli, Italy
[d] Dipartimento di Scienze della Vita e dell'Ambiente, Marche Polytechnic University, Via Brecce bianche, 60131 Ancona, Italy

ARTICLE INFO

Article history:
Received 16 November 2015
Received in revised form 6 June 2016
Accepted 22 June 2016
Available online 26 June 2016

Keywords:
Particulate organic matter
Biochemical composition
Phytoplankton biomass
Physical structure
Ross Sea
Antarctica

ABSTRACT

The 0–200 m surface layer of the Ross Sea was studied during summer 2014 to investigate the lability of the particulate organic matter (POM) in response to physical parameters. With the use of satellite information, we selected three zones, characterised by different physical setting: a northern offshore area, crossing the summer-polynya area of the Ross Sea (hereafter called ROME 1), a more coastal area next to the Terra Nova Bay polynya (ROME 2); a southern offshore area, towards the Ross Ice Shelf (ROME 3). Ice-maps showed that the seasonal ice retreat had already occurred in early December for most of the stations. Statistical analysis of the quantitative and qualitative characteristics of the POM pointed to significant differences between the stations, especially in the upper mixed layer (UML). A comparison with previous studies showed that the localised pulses of POM accumulation in the UML were similar to those recorded at the highly productive marginal ice zones, providing notable trophic support to the ecosystem. The UML, although rather thin and easily subjected to alterations, confirmed its pivotal role in the ecosystem dynamics. A POM quality favourable to consumers was highlighted at several stations in ROME 1 and ROME 3. Reduced trophic support was, instead, found in ROME 2. Limited POM consumption where deep-water formation takes place would increase the POM role in the transfer of C to the depths.

1. Introduction

Particulate organic matter (POM) is operationally defined as any material that does not pass through a given filter, usually 0.45–1 μm (Volkman and Tanoue, 2002; Verdugo et al., 2004). POM includes detrital matter as well as living organisms. Ice-algae, phytoplankton, nano- and microzooplankton, and mesozooplankton-derived particles are included in POM, as well as bacteria adhering on particles.

In the Antarctic Ocean, the quantitative features of the POM have been extensively studied using in-situ bottle and pump sampling and remote-sensing techniques (especially chlorophyll-a and particulate organic carbon - POC) (e. g. Smith et al., 2000; Smith and Asper, 2001; Lee et al., 2012; Arrigo et al., 2012; Schine et al., 2016), while detailed information on its biochemical composition and nutritional value for consumers is less abundant (e. *G. Rossi* et al., 2013; Soares et al., 2015; Kim et al., 2016).

In addition to the ratios that are commonly used to infer the value of POM as a trophic resource (for instance the POC/PON ratio and the POC/chlorophyll-a ratio), other analyses focusing on the caloric content and hydrolysable fractions of the POM can be useful (Fabiano et al., 1993; Fabiano and Pusceddu, 1998; Misic and Covazzi Harriague, 2008; Kim et al., 2014). Caloric content expresses the general value of POM in energy terms. Different biochemical compositions result in quantitatively different energy values for POM. For the hydrolysable fraction, potential biomimetic assays have been developed to evaluate the fraction that may be rapidly hydrolysed by enzymes commonly found in the environment; these assays estimate the actual fraction of POM that is bioavailable to consumers. This approach, although testing only a few of the enzymes actually active in the environment, by-passes the uncertainty of bulk-related analyses (such as POC). The biomimetic assay allows for the possibility that some compounds may be biochemically refractory to consumption, or physically enclosed in low-lability materials that isolate them from consumers.

The Antarctic Ocean and the Ross Sea are characterised by interannual, seasonal and spatial variability of biological features (Smith et al., 1996; Arrigo et al., 1998; Dunbar et al., 1998; Gardner

* Corresponding author.
E-mail address: misic@dipteris.unige.it (C. Misic).

http://dx.doi.org/10.1016/j.jmarsys.2016.06.012
0924-7963/

et al., 2000; Saggiomo et al., 2002; Smith et al., 2010; Fragoso and Smith, 2012), whose forcing mechanisms are still largely unclear. Among others, the ice presence regulates the onset of primary production, POM accumulation and distribution in the water column (Garrity et al., 2005). The ice presence or absence influence the water column properties, determining the depth of the upper mixed layer (UML) that is often considered to be a major factor in controlling POM production and distribution (Mangoni et al., 2004; Fragoso and Smith, 2012). Therefore, based on the degree of maturity of the selected ice-system, a typical evolution scheme may be defined (Fabiano et al., 2000): closed pack conditions, followed by the Marginal Ice Zone (MIZ) spring conditions, and then by open waters in late spring and summer. This occurs, generally in the offshore area by late December and in the entire continental shelf region by late January (Comiso et al., 1993; Smith and Asper, 2001). Once the ice is melted in summer, other forces can influence the planktonic patterns. Although ice may last longer at some sites in the Ross Sea, depending on global climate anomalies as well as local events (Arrigo and van Djiken, 2004), the summer features of the Ross Sea should show less variability than the spring ones. The stratification generated by ice melting should be relaxed due to wind and waves on the open waters, a feature that would allow increased vertical water mixing and a more homogeneous vertical distribution of the POM (Gardner et al., 2000).

This study is based on the results of the ROME (Ross Sea Mesoscale Experiment) cruise, carried out during the Antarctic summer of 2014. Sampling focused on the 0–200 m surface layer of three locations in the Ross Sea, characterised by different distances from the coast and different mesoscale hydrodynamic structures.

We aimed to: i) highlight whether the quantitative and qualitative features of the POM were homogeneous and the potential effects of physical constraints in the sampled areas, ii) test whether our summer POM features resembled those of previous research performed in the Ross Sea, iii) underline the potential role of the POM as trophic resource.

2. Material and methods

2.1. Station sites and sampling

The in situ ROME data were collected by the R/V Italica in the framework of the Italian National Program for Antarctic Research (PNRA). Sampling was performed in three different areas of the Ross Sea: ROME 1 was sited at approximately 170°E and 75°S; ROME 2 occupied a more coastward area, next to the Terra Nova Bay (TNB) polynya; ROME 3 was placed in the southern Ross Sea, towards the Ross Ice Shelf, at ca. 168°E (Fig. 1A).

The sampling strategy was defined using sea surface temperature and surface chlorophyll-a concentration maps from MODIS (Moderate Resolution Imaging Spectroradiometer) Aqua and Terra satellite level-2 products for the previous 12/24 h. The goal was to carry out bottle casts where both high and low chlorophyll occurred. Additionally, satellite AMSR2 sea ice concentration maps, provided by the University of Bremen, using the ASI sea ice concentration algorithm (Spreen et al., 2008), were considered. Daily maps of the Ross Sea region from early December 2013 to late February 2014 (available at http://www.iup.uni-bremen.de:8084/amsr2) were analyzed to monitor the evolution of the sea ice cover before and during the experiment.

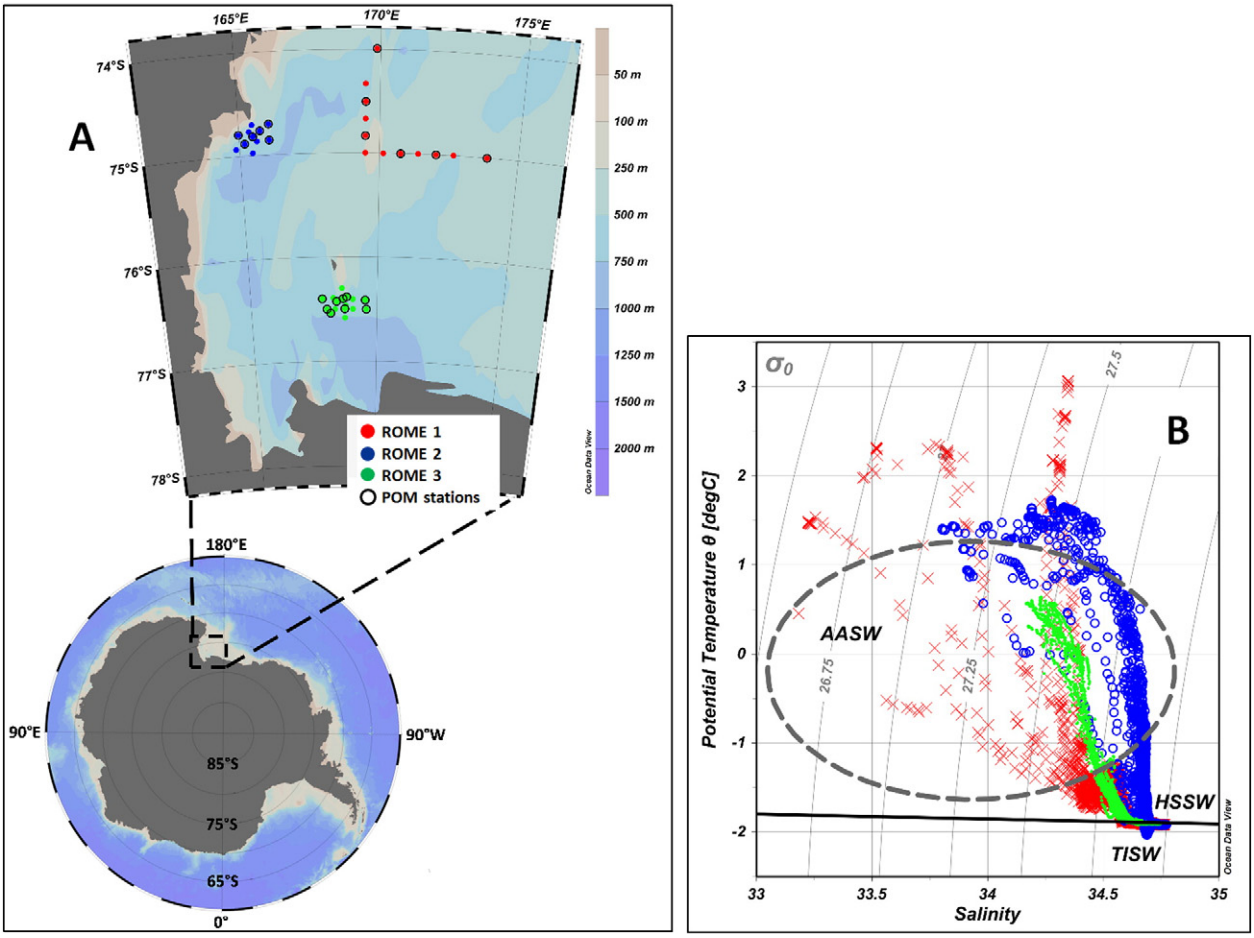

Fig. 1. A: Map of the stations of the ROME 1 (red dots), ROME 2 (blue dots) and ROME 3 (green dots) areas. Black-circled points indicate the POM sampling stations. B: Θ/S diagram obtained from the entire available dataset indicates the main water masses. Data from the three different areas (ROME 1, ROME 2 and ROME 3) are represented with different colours (red, blue and green, respectively).

A total of 46 casts were conducted. Hydrological profiles were acquired by means of a SBE 9/11 Plus CTD, with double temperature and conductivity sensors. For each station the upper mixed layer (UML) depth was determined as the depth at which in situ density (σ_t) changed by 0.05 kgm^{-3} over a 5 m depth interval. Current speed and direction were recorded using a Lowered Acoustic Doppler Current Profiler (LADCP) system. Two LADCP were deployed with the CTD, in order to obtain a unique current measurement every 10 m from the surface to the maximum depth reached. The effect of tides on the current dataset was removed following the procedure proposed by Erofeeva et al. (2005).

Water samples for phytoplankton biomass and POM analysis were collected at 21 stations (Table 1, black circled stations in Fig. 1A) using a Carousel sampler equipped with 24 Niskin bottles (12 l).

For the POM analysis, water samples were collected at 4 fixed depths (surface, 50, 100 and 200 m) and 1 variable depth depending on the maximum of the signal for fluorescence. From 0.5 to 1 l of sampled seawater was filtered through Whatman GFF filters (25 mm, nominal pore diameter 0.7 μm) and immediately frozen until analysis in the laboratory. For the total phytoplankton biomass analysis, the samples were filtered and quickly stored at −80 °C.

2.2. Analytical procedures

The amount of phytoplankton biomass was estimated from spectrofluorometric analysis on acetone-extracted chlorophyll-a, following Holm-Hansen et al. (1965). The extract was read using a Varian Eclipse spectrofluorometer, which was checked daily with a chlorophyll-a standard solution (from *Anacystis nidulans* by Sigma). The specific standard deviation of the replicates was based on an average of 4%.

Particulate organic carbon (POC) and particulate organic nitrogen (PON) were analyzed following Hedges and Stern (1984), after acidification with HCl fumes, in order to remove inorganic carbon. Cyclohexanone 2–4-dinitrophenyl hydrazone was used to calibrate a Carlo Erba Mod. 1110 CHN Elemental Analyser. The specific standard deviations due to the analytical procedures and sample handling were 7.4% and 7.8% for POC and PON, respectively.

Particulate protein, carbohydrate and lipid concentrations were analyzed following Hartree (1972); Dubois et al. (1956); Bligh and Dyer (1959) and Marsh and Weinstein (1966). Albumin, glucose and tripalmitine solutions were used to calibrate a Jasco V530 spectrophotometer. The specific standard deviations were 8.3%, 15.5% and 21.6% for the proteins, carbohydrates and lipids, respectively.

The concentrations of proteins, carbohydrates and lipids were used to estimate the caloric value of the POM (Kcal g POM^{-1}) following the Winberg (1971) equation (Kcal g POM^{-1} = 0.055 protein% + 0.041 carbohydrate% + 0.095 lipid%).

The enzyme-hydrolysable fractions of particulate proteins and carbohydrates were determined following the protocols of Gordon (1970); Mayer et al. (1995) and Dell'Anno et al. (2000). The sample filters and filter blanks (Whatman GFF filters not used for filtration) were placed in plastic containers with solutions (100 mg l^{-1} in 0.1 M Na-phosphate buffer) of two selected enzymes purchased from Sigma–Aldrich. Proteinase K was chosen for the hydrolysis of the proteins, β-glucosidase for that of the carbohydrates (Mayer et al., 1995; Dell'Anno et al., 2000). These enzymes are extracted from plants and fungi, but have hydrolytic activities quite similar to natural marine organisms and are widespread among autotrophs and heterotrophs (Dall and Moriarty, 1983). The filters were left in the enzyme solutions for 2 h, at the optimal temperatures and pH for each enzyme, in order to enhance digestion (Dell'Anno et al., 2000). After hydrolysis, each filter was carefully removed from its container, placed in a filter-holder and rinsed with the solution remaining in the dish and 5 ml of deionised water, to return any particles that may have floated off the filter (Gordon, 1970). After that, the filters were processed for determinations of protein and carbohydrate concentrations as above. The possibility that the flushing of the buffer could have mechanically removed part of the particulate fraction was avoided by incubating and processing replicates of the samples with only the buffer solution. In addition, an underestimate of the labile proteins and carbohydrates was possible due to the sorption to minerals or POM (and therefore to their return to the particulate fraction) of the hydrolysed materials. The concentrations detected after hydrolysis, corrected for the eventual error just mentioned (never higher than 20% of the total protein and carbohydrate concentrations), were subtracted from the total concentrations in order to obtain the hydrolysable, or labile, POM. The specific standard deviations were 11.2% and 21.5% for hydrolysable particulate proteins and carbohydrates, respectively.

2.3. Data treatment and statistical analysis

The POM data were divided into a surface layer, defined by the UML depth (Table 1), and a deeper layer, ranging from the UML depth down to 200 m.

Published data related to previous researches carried out in the Ross Sea and TNB were used for comparison. In particular, POC, protein and

Table 1
Position of the stations sampled for POM characterisation during the ROME cruise in 2014, depth of the upper mixed layer (UML) and number of sampled depths for each station.

	Station	Date	Longitude (°E)	Latitude (°S)	UML depth (m)	Sampled depths
ROME 1	9	16 Jan	173.87	75.00	38	5
	11	16 Jan	172.03	75.00	29	5
	13	16 Jan	170.76	75.00	32	5
	16	17 Jan	169.50	74.83	15	5
	18	17 Jan	169.51	74.51	17	5
	20	17 Jan	169.88	73.99	14	5
ROME 2	33	26 Jan	166.06	74.70	18	4
	34	26 Jan	165.75	74.76	13	5
	36	27 Jan	165.18	74.88	12	5
	39	27 Jan	166.06	74.86	24	4
	43	27 Jan	164.98	74.79	14	4
	45	28 Jan	165.49	74.82	15	5
ROME 3	48	31 Jan	167.83	76.40	33	5
	50	31 Jan	168.65	76.40	36	5
	52	1 Feb	169.53	76.42	75	4
	55	1 Feb	168.40	76.43	44	5
	56	1 Feb	168.16	76.54	12	5
	65	2 Feb	169.58	76.50	115	4
	67	2 Feb	168.72	76.50	51	5
	69	2 Feb	168.01	76.50	14	4
	75	3 Feb	168.80	76.38	42	5

carbohydrate spring concentrations for the Ross Sea were provided by Fabiano et al. (2000), while early summer data were found in Fabiano et al. (1993) and Catalano et al. (1997). Summer data for the TNB area have been published by Fabiano et al. (1995, 1997) and Povero et al. (2001) (Table 2).

We tested the significance of differences in each variable between different samplings with the one-way ANOVA test followed by the Newman-Keuls *post-hoc* test (ANOVA-NK test) (Statistica software). To test the relationships between the various parameters, a Spearman-rank correlation analysis was performed.

Principal Component Analysis (PCA) was applied to the normalised POC, protein and carbohydrate concentrations and the protein/carbohydrate ratio (PRIMER software). The data were divided into the UML and the deeper layer, as previously described. The ROME data were treated together with the other literature data previously cited (Table 2) to highlight similarities between them. Cluster analysis was performed on the normalised data set (resemblance measure: Euclidean distances, cluster mode: group average), to visually highlight the station grouping. The analysis of similarities (ANOSIM) was applied to highlight significant differences between the groups, while the similarity percentage analysis (SIMPER) was utilised to highlight the parameters responsible for such differences.

3. Results

3.1. Physical properties and sea-ice conditions

The Θ/S diagram obtained from all the sampled stations (Fig. 1B) indicated the presence of several typical Ross Sea shelf water masses. In all the studied areas the surface layer was occupied by Antarctic Surface Water (AASW), a relatively light surface water characterised by potential temperatures ranging between −1.8 °C and +1 °C and by salinity values lower than 34.50 (Orsi and Wiederwohl, 2009). In ROME 2 (blue circles in Fig. 1B), the AASW core was slightly saltier and denser than expected, with salinity close to 34.60. These values were similar to the Modified Circumpolar Deep Water (MCDW) features, but the high oxygen concentration values (Rivaro et al., 2017) confirmed that we were in the presence of a local AASW.

The intermediate and deep layers (from 150 to 1000 m) were occupied by High Salinity Shelf Water (HSSW) and by Terra Nova Bay Ice Shelf Water (TISW), the latter identified only in ROME 2 (Fig. 1B). HSSW is characterised by salinity >34.70, potential temperature near the freezing point and potential density >27.9 kg/m^3 (Budillon et al., 2003; Rivaro et al., 2014). TISW (from 150 to 350 m) is characterised by potential temperatures below freezing point and salinity values of about 34.70 (Budillon and Spezie, 2000).

The physical properties of the upper layer may also be linked to sea ice evolution in the study area. The melting ice in the Ross Sea gradually generates large ice-free areas during summer. Some ROME 1 and ROME 3 stations and all the ROME 2 stations experienced ice-free conditions starting from early December (Fig. 2A and B). On the other hand, some stations experienced a longer ice presence (Fig. 2C and D). Even in the same sampling area, differences in ice cover can be significant and have an impact on the observed temperature and salinity values. For instance, the northernmost station of ROME 1 (station 20) was covered by ice until 14 January, just 3 days before the sampling. Stations 16 and 18 started to become ice-free from the beginning of January (Fig. 2C). The ROME 3 stations were partially covered by ice just until the end of December (Fig. 2B).

The vertical structure of the water column of ROME 1 showed deeper UMLs for the stations that experienced longer ice-free conditions (9, 11 and 13, Table 1). In the western stations of ROME 1 the lower depth of the mixed layer depended on the presence of low-salinity surface water, related to the influence of the ice (Fig. 3A). Intensity and direction of the currents along the entire water column (mean UML shown in Fig. 3C) showed the presence of a northward current along the eastern and western boundary of the leg, while more intense southward velocities were registered in the central part of the leg (stations 13 and 14).

The ROME 2 water column was characterised by a UML depth limited to the first 10–15 m (Table 1) due to the presence of a salinity and temperature gradient between the fresher and colder coastal stations and the easternmost, saltier and warmer stations (Fig. 3D and E). A frontal structure was visible in the area between stations 45 and 34, where the convergence of the two water masses led to a deepening of the thermocline down to 100 m (Rivaro et al., 2017) and to an abrupt change in the current pattern (Fig. 3F).

The strongest current intensities ($p < 0.05$) were observed in ROME 3, with values up to 24 cm sec^{-1} for the zonal (u) and meridional (v) components. The current pattern at all depths showed the presence of a cyclonic circulation centred at about 168.5°E 76.45°S (Fig. 3I). This circulation could have increased the UML water mixing, leading to salinity values of 34.23–34.43 and mean temperature values lower than 0.5 °C (Fig. 3G and H). In fact, the western and central stations (48, 50, 55, 67 and 75) had a more homogeneous water structure for the upper 30–50 m, while stations, placed outside the eddy showed higher surface salinity values and the deepest UML (>70 m).

Table 2
Features of the stations sampled during previous researches, here used as a comparison for the ROME cruise observations.

Area	Season	Environmental features	Station	Lat °S	Long °E	Reference
Ross Sea	Spring	Polynya	MP	76.50	175.00	Fabiano et al. (2000)
		MIZ	8	75.16	175.18	
		MIZ	10	74.84	174.88	
		MIZ	28	74.70	172.01	
		MIZ	30	74.69	164.18	
		Pack	27	71.94	174.98	
		pack	29	74.98	167.99	
	Early summer	Polynya	15	72.35	179.78	Fabiano et al. (1993); Catalano et al. (1997)
		Polynya	17	73.23	179.84	
		Polynya	19	74.95	179.82	
		Polynya	21	74.98	174.87	
		MIZ	23	74.99	170.00	
		MIZ	25	74.95	165.25	
Terra Nova Bay	Summer	Coastal-open waters	TNB	74.78	164.17	Povero et al. (2001)
			TNBa	74.75	164.17	Fabiano et al. (1995)
			TNBb	74.70	164.13	Fabiano et al. (1997)

3.2. Particulate organic matter

The concentration and distribution of chlorophyll-a in the three areas (see Table in appendix) varied with the physical setting. In ROME 1 the stations characterised by early ice melting showed rather homogeneous chlorophyll-a concentrations in the UML, ranging from 1 to 2 μg l^{-1}. Instead, where the halocline was shallower and the stratification stronger (i.e. station 16), a subsurface increase in concentration up to 3 μg l^{-1} was observed, leading to higher average values. The chlorophyll-a distribution in ROME 2 was influenced by the previously described hydrological front (Fig. 3D and E), associated with the deepening of the thermocline at stations 34 and 45. The frontal structure and the current convergence allowed high chlorophyll-a concentrations at higher depths (values up to 3 μg l^{-1} at 100 m, data not shown). In ROME 3 the stations directly influenced by the cyclonic eddy (55, 67 and 75) showed the highest mean chlorophyll-a concentrations, with maximum values higher than 4 μg l^{-1}.

POC values correlated significantly with chlorophyll-a concentrations in ROME 1 and ROME 3 (Table 3). ROME 2, instead, showed no significant correlation, although at 50 and 100 m depths significantly

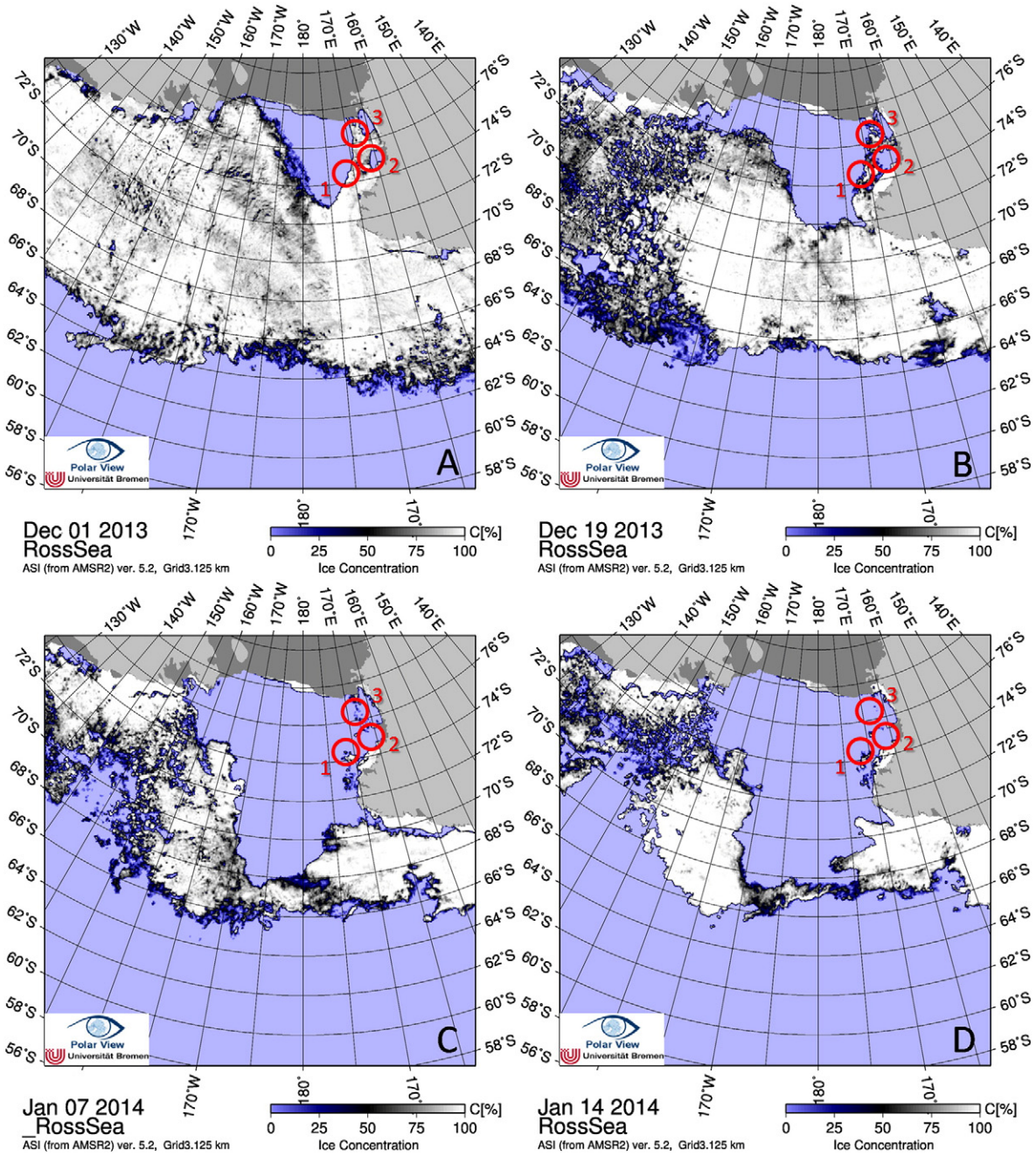

Fig. 2. Sea-ice concentration maps of the Ross Sea for 1 December (A), 19 December (B), 7 January (C), 14 January (D). Red circles and numbers highlight the position of the ROME 1, ROME 2 and ROME 3 sampling areas.

higher POC concentrations ($p < 0.05$) than the other two areas were found (Fig. 4A).

The POC/chlorophyll-a ratio is an indication of the primary biomass contribution to the total POM. The ratios (see Table in appendix) highlighted a generally lower contribution of the photoautotrophic component at the UMLs of ROME 1 and 2, with ratio higher than 150, especially in the stations experiencing longer ice-free conditions (stations 9 and 11 of ROME 1, for instance). In ROME 3 the lowest ratio was, instead, found for the stations lying to the west of the frontal zone.

PON and POC concentrations were strongly correlated (Table 3), indicating similar distributions (Fig. 4A and B) and likely origins. POC/PON ratios showed variations with depth (Fig. 4C); this ratio gives an estimate of the N contribution to the bulk POM, an indication of lability given that *N*-containing molecules are considered attractive to consumers. The highest POC/PON ratios (above 8) were found in the deeper water layers, especially at stations 9 and 11 in ROME 1 and 50, 52, 56, 69 and 75 in ROME 3. The lowest values, below 6, were, instead, found in the UML, especially in ROME 3, where the highest chlorophyll-a values were found. However, significant chlorophyll-a and POC/PON ratio correlations were only found in ROME 2, although this relationship ($r = 0.48$, $n = 19$, $p < 0.05$) highlighted that an increase of autotrophic biomass led to a lowering of the trophic value of the POM.

On average, the protein and carbohydrate concentrations showed vertical trends very similar to those of POC (Fig. 4D and G), and significant correlations were found between these variables for the three areas (Table 3). Proteins and carbohydrates also correlated with chlorophyll-a

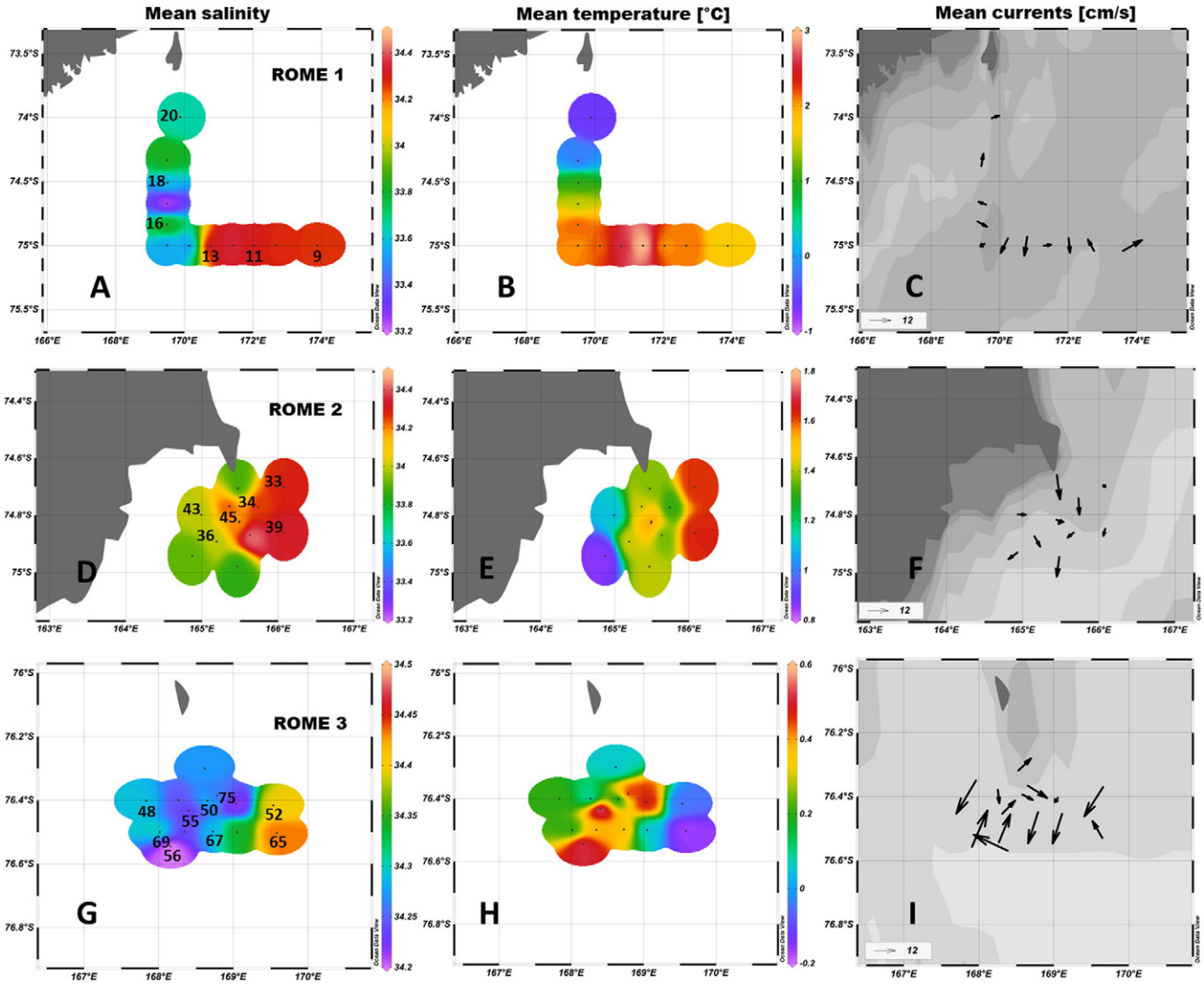

Fig. 3. Salinity (left column), temperature (central column) and measured currents (right column) in the upper mixed layer for ROME 1 (A,B,C), ROME 2 (D,E,F) and ROME 3 (G,H·I).

in ROME 1 and 3, while no significant correlation was found in ROME 2. Furthermore, the hydrolysable fraction of the carbohydrates and lipids was not coupled with the other variables in ROME 2. A reduction of the hydrolysable carbohydrates was, in fact, observed starting from 100 m (Fig. 4H). In this area the lipid concentrations (Fig. 4I) did not show significant decreases with depth (UML vs. deeper layer, $p > 0.05$) but rather similar values, significantly lower than in the other areas ($p < 0.001$). The contribution of the three POM fractions to POC was reported in Fig. 5A for the UML and the deeper layer. Generally, higher concentrations of residual POC (here called "other POC") were found at the UML, except for stations 34 and 45, that showed a high residual POC fraction also in the deeper layer.

On average, the hydrolysable proteins were 35.4 ± 11.7% of the total proteins (ranging from 6.8 to 75.6%), the hydrolysable carbohydrates 13.1 ± 10.8% of the total carbohydrates (ranging from 0.1 to 44.9%). Generally, the deeper layer contribution of the hydrolysable proteins to POC was higher than the UML one, except for the front-related stations in ROME 2 and station 20 in ROME 1 (Fig. 5A). The hydrolysable carbohydrate contribution to POC (Fig.5B) was lower and showed a higher variability in the three areas. In ROME 1, for instance, the contribution showed an inverse trend with chlorophyll-a. The 200-*m*-deep contributions were higher at the stations not covered by ice from a longer time, than at the stations more recently influenced by ice. ROME 3, however, showed a rather good relationship between the hydrolysable carbohydrate and the phytoplanktonic biomass. The large variability of the hydrolysable carbohydrate contribution to the POC concentration, often visible in Fig. 5B as high standard deviation, implied also strong variations within the UML and the deeper layer that were not found for the hydrolysable proteins.

3.3. Multivariate statistical analysis

PCA results are shown in Fig. 6, where the cluster analysis is shown as ellipses defined by Euclidean distances. The PC1 axis explained 71% of the variation, while the PC2 explained a further 24%. Two significantly different main groups (ANOSIM analysis, Table 4) were observed: the main part of the UML observations belonged to the richer group A, while the deeper layer observations were clustered in group B. Proteins and carbohydrates explained the major part of this difference (SIMPER analysis, Table 4). The group B stations showed POC concentrations 3.4-fold lower than the observations of group A, 4.8 for proteins and 2.8 for carbohydrates.

In group A the samples were organised into two main sub-groups: a1 and a2. The multivariate analyses highlighted significant differences between them (ANOSIM analysis, Table 4), mainly due to the different ratios between proteins and carbohydrates (explaining 41% of the

Table 3
Significant correlations between the different variables for each area investigated during the ROME cruise. Underlined numbers: $p < 0.05$, normal numbers: $p < 0.01$, bold numbers: $p < 0.001$. The number of observation varied in the three Legs: in ROME 1 chlorophyll-a showed 13 observations, hydrolysable carbohydrate and lipid 18, the other variables 28. In ROME 2 they were: 19, 12 and 25, respectively. In ROME 3: 25, 13 and 40, respectively.

		Chl-a	PON	POC	PRT	h-PRT	CHO	h-CHO
ROME 1	PON	0.68						
	POC	0.72	**1.00**					
	prt	0.73	**0.99**	**1.00**				
	h-PRT	0.76	**0.94**	**0.95**	**0.97**			
	CHO	0.71	**0.97**	**0.98**	**0.98**	**0.94**		
	h-CHO	–	**0.76**	**0.75**	**0.77**	**0.83**	**0.82**	
	LIP	*0.63*	**0.89**	**0.92**	**0.91**	**0.90**	**0.88**	0.65
ROME 2	PON	–						
	POC	–	**0.96**					
	prt	–	**0.97**	**0.95**				
	h-PRT	–	**0.89**	**0.90**	**0.94**			
	CHO	0.65	**0.68**	**0.81**	**0.77**	**0.79**		
	h-CHO	–	–	–	–	–	0.72	
	LIP	–	–	–	–	–	*0.53*	*0.63*
ROME 3	PON	**0.95**						
	POC	**0.95**	**0.99**					
	prt	**0.95**	**0.99**	**0.99**				
	h-PRT	**0.86**	**0.93**	**0.94**	**0.94**			
	CHO	**0.90**	**0.93**	**0.95**	**0.94**	**0.91**		
	h-CHO	*0.64*	0.74	0.74	0.74	0.72	**0.80**	
	LIP	0.68	**0.91**	**0.91**	**0.90**	**0.90**	**0.89**	0.68

Chl-a: chlorophyll-a, PON: particulate organic nitrogen, POC: particulate organic carbon, PRT: proteins, h-PRT: hydrolysable proteins, CHO: carbohydrates, h-CHO: hydrolysable carbohydrates, LIP: lipids.

difference, SIMPER analysis, Table 4). In group B two more sub-groups were recorded, differing significantly (ANOSIM analysis, Table 4) due to the carbohydrate concentrations (explaining 47% of the difference, SIMPER analysis, Table 4).

Each sub-group had a particular signature, defined by the previous studies carried out in the area (Table 2): sub-group a1 clustered the MIZ stations (8, 10, 28, 30) and the spring polynya station MP, sub-group a2 the coastal TNB stations. The surface observations characterised by a closed-pack coverage (27 and 29) belonged to sub-group b1, together with the main part of the deeper layer observations; sub-group b2 collected those of the early summer polynya stations (15, 17, 19, 21) and the deeper coastal layer observations (TNB).

3.4. Caloric value analysis

The caloric value of the POM in the two water layers was only calculated for stations where the lipid analysis was carried out, namely 9, 13, 16 and 20 of ROME 1, 34, 39 and 45 of ROME 2 and 50, 55 and 67 of ROME 3. The plot of these results, with the previous research carried out in the Ross Sea and at the coastal TNB (Table 2) is presented in Fig. 7. In this figure we have merged the bulk quantitative (POC) and qualitative (caloric value) information on the POM.

During previous research (Fabiano et al., 2000), a rising trend was noticed for POM concentrations in the UML from the poorer pack-ice zones to the polynya and then to the MIZ, ending with the richer coastal sites, although the MIZ could also show high concentrations of POM of moderate caloric values. The previous pack-ice observations (Fabiano et al., 1993) showed that low concentrations were associated with an average caloric value, while the qualitative value of the other stations was higher (MIZ and coastal) or lower (polynya).

The stations in ROME 2 matched the quantitative and qualitative features of the polynya in the entire water column. The surface observations of the other areas were grouped with the MIZ and previous coastal observations for the UML. The deeper layer observations in the ROME 1 and ROME 3 areas resembled those of the MIZ, spring polynya and deeper pack-layer, although their caloric value was higher.

4. Discussion

4.1. Quantitative and qualitative features of the summer POM and a comparison with previous studies in the Ross Sea

Focusing on the quantitative characteristics of POM at different stations (PCA -multivariate analysis, Fig. 6), we observed significant quantitative differences between the two water layers (Table 4), with a sharp reduction in POM in the deeper layer, as already established by the observations by Nelson et al. (1996); Fabiano et al. (2000) and Gardner et al. (2000) for the Ross Sea. They stated that the primary production is recycled in the photic layer, following the concept of a "retentive system". The grouping of the observations of the two layers, as revealed by multivariate analysis, indicated a strong and significant variability in the UML, while the deeper layer was more homogeneous in the ROME study area, also when compared to observations from other years and seasons, except for the ROME 2 stations influenced by the frontal area.

Ice-free water conditions were established in the whole ROME sampling area from the beginning of January (with the exception of the northern station of ROME 1), at least two weeks before the sampling. Therefore, open water conditions, resembling those of the previous spring-summer polynya/open water observations, were common in the entire area. Actually, the multivariate analysis performed on the UML POM indicated a higher similarity to the spring MIZ zones studied in the previous published researches than to the summer polynya ones. Several processes, due to the peculiar physical features as well as biological, may be responsible of such similarity, irrespective of the ice dynamics.

In our study, an example of the strict relationship between physical forcing, phytoplankton biomass and POM accumulation was provided by ROME 3, where a clear cyclonic circulation was observed. In this case, the UML depth (generally deeper than 30 m in our study) exerted a lower influence on the POM production and accumulation than that observed by Fragoso and Smith (2012), who noted that the shallower mixed layer depths (<20 m) in late spring and early summer appeared to promote diatom growth. In our study, the water mixing of the UML, due to the more intense hydrodynamic forcing, fertilised the surface layer, probably stripped of nutrients by earlier spring blooms. In addition, a higher instability in the water column, that is known to influence phytoplankton development, could have favoured some species that, before, were limited by competition (Fonda Umani et al., 2002).

The phytoplankton biomass was pivotal for the POM composition. In fact, it regulated the POM quantitative features, as revealed by the highly significant correlations between the chlorophyll-a and the quantitative variables of the POM (Table 3) (Davis and Benner, 2005) and by the POC/chlorophyll-a ratio values for the stations on the western side of the area (eddy-influenced zone), that were significantly lower ($p < 0.05$) than the other ROME areas. Young et al. (2015) found that Antarctic diatoms take up to 50% of biomass to protein, explaining the very high significance of the correlation. Arrigo and van Djiken (2004) described the area of ROME 3 as a boundary between spring and summer blooms, a kind of frontal area that may show an unusually high chlorophyll-a accumulation at the surface, depending on general atmospheric conditions over the entire Ross Sea.

Our observations point to the pivotal role of the summer autotrophic processes, providing a large accumulation of biomass and strongly sustaining the ecosystem. This feature was unclear in the multi-year

Fig. 4. Vertical profiles of the variables averaged for each depth at each area (standard deviations are reported). A: particulate organic carbon (POC), B: particulate organic nitrogen (PON), C: particulate organic carbon/particulate organic nitrogen ratio (POC/PON), D: particulate proteins (PRT), E: hydrolysable particulate proteins (h-PRT), F: particulate proteins/carbohydrate ratio (PRT/CHO), G: particulate carbohydrates (CHO), H: hydrolysable particulate carbohydrates (h-CHO), I: particulate lipids (LIP).

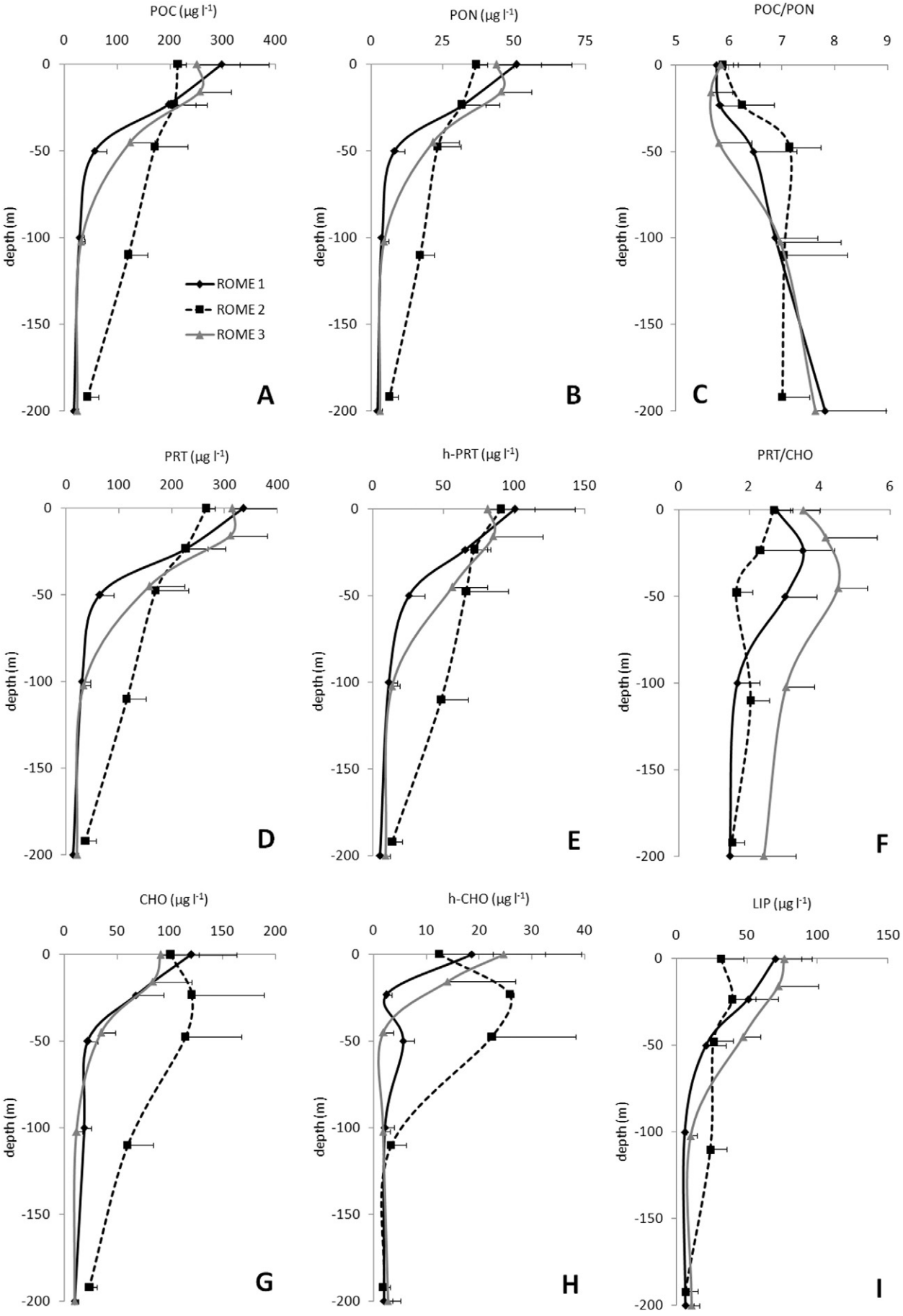
POC (µg l-1)
PON (µg l-1)
POC/PON
PRT (µg l-1)
h-PRT (µg l-1)
PRT/CHO
CHO (µg l-1)
h-CHO (µg l-1)
LIP (µg l-1)
depth (m)
ROME 1
ROME 2
ROME 3
A
B
C
D
E
F
G
H
I

comparison by Arrigo and van Djiken (2004) and in the studies by Smith and Asper (2001) and Rigual-Hernández et al. (2015), who observed a general decrease in chlorophyll-a concentrations from spring to summer in normal years. In addition, the POC/chlorophyll-a ratios of our study were significantly lower ($p < 0.05$) than those reported by Smith et al. (2000) for the Ross Sea in summer, while they were similar to the values the same authors reported for spring. This confirmed the pivotal role of the living phytoplankton fraction during summer in the UML of the Ross Sea, where mesoscale hydrological structures occur.

The sub-group a1 of the PCA linked some stations of the ROME cruise and the previously studied spring polynya station MP and spring MIZ ones. The MIZ stations are generally characterised by high POM productivity (Saggiomo et al., 1998; Fitch and Moore, 2007), being the priming for further planktonic development. The multivariate statistical analysis confirmed that these stations had rather high POM concentrations and, in particular, they showed the highest prevalence of proteins over carbohydrates, a signal of recent production (Pusceddu et al., 2000). It is well known that *N*-rich proteins cover multiple roles (energetic, functional, structural) and thus a high protein concentration indicates a good food supply for consumers (Etcheber et al., 1999), especially in the upper water column. Particulate carbohydrates, instead, generally have a lower lability, because they also encompass complex structural polysaccharides whose digestion is energy-expensive, slowing their consumption rates (Pusceddu et al., 2000). One of the main processes that enrich the POM of proteins is microbial activity. Microbial heterotrophic reworking of autotrophic and detrital POM, generally performed by bacteria, increases the N content of the detritus (Povero et al., 2003) and of the autotrophic colonies (Carlson et al., 1998) especially during summer. A general and marked dominance of proteolysis over other classes of hydrolytic enzymes has been previously reported (Misic et al., 2002; Celussi et al., 2009), indicating an efficient *N*-recycling by unicellular heterotrophs. The conversion of detrital-N into high trophic value biomass is completed by an efficient microbial-loop, recovering a large part of the DOM released during phytoplanktonic blooming (Kirchman et al., 2001). In addition, Sala et al. (2005) found that bacteria might utilise other DOM sources (in particular dissolved carbohydrates), thus increasing their efficiency in biomass accumulation. The rather low POC/PON ratio values we found compared, for instance, to Smith et al. (2000) (on average for the upper 100 m layer they found summer values of 6.9 ± 0.5 vs. our 5.8 ± 0.3 and 6.4 ± 0.9 calculated for the UML and 0–200 m layer, respectively), are consistent with micro-heterotrophic presence, as bacterial standing stock can be considered as the amount of particulate organic matter possessing high nutritional quality (Monticelli et al., 2003).

4.2. Caloric value of summer POM

The plotting of the POC with the POM caloric value (Fig. 7) provides information on the energy potentially available for the heterotrophic consumers by the POM. The ROME stations that resemble the spring and early-summer features of the polynya were those of ROME 2. Actually, these stations experienced real polynya environmental conditions, being next to the TNB polynya.

The ROME 2 stations had low caloric values in the entire water column, although, from a quantitative point of view, some of them in the UML had similar features to the richer coastal areas (sub-group a2 of Fig. 6). In the entire water column, POM maintained the same caloric content of the mixed layer, as previously found for the coastal TNB (Fabiano et al., 1996), when the caloric value was on average 5.33 Kcal/g. This is not really very high, due to the high contribution of carbohydrates that have the lowest caloric value among the three biochemical components. We observed that in ROME 2 the chlorophyll-a was associated with carbonaceous POM (it correlated positively to the POC/PON ratio), therefore in this area the freshly-produced summer POM had different features, namely a lower trophic value, than the offshore area.

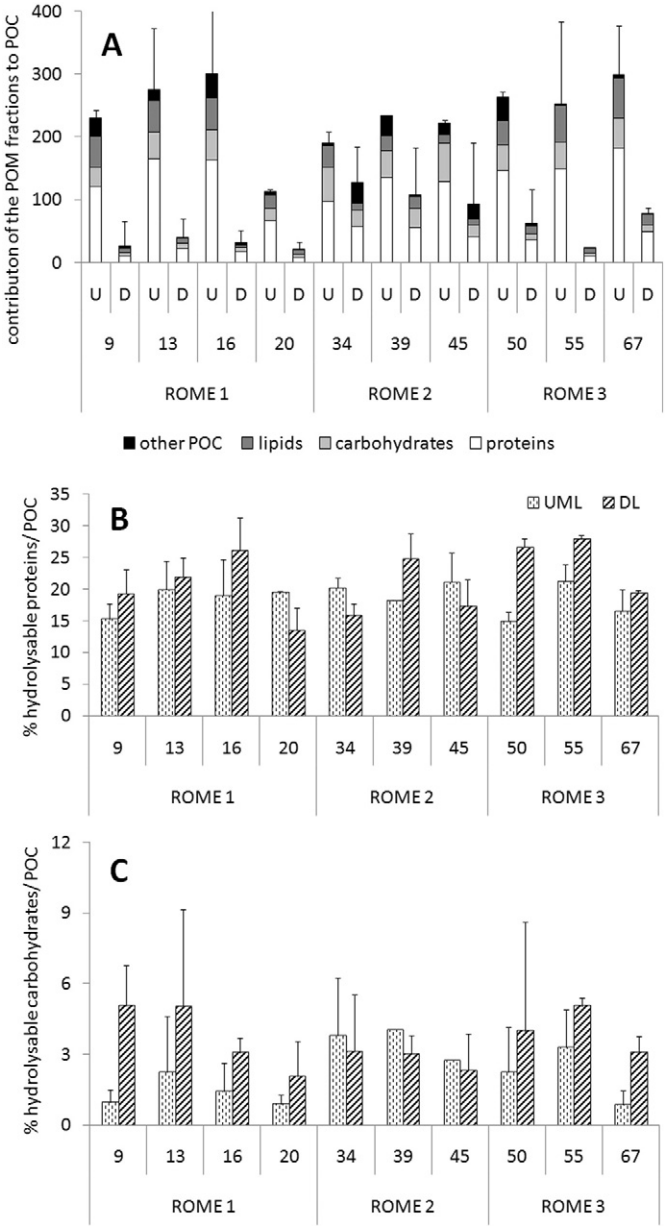

Fig. 5. (A) Contribution of proteins (white), carbohydrates (light grey) and lipids (grey) to POC in the UML (U) and deeper layer (D) for ROME 1, ROME 2 and ROME 3 areas. Black indicates the non-identified fraction of POC, here called "other POC". (B) Average contribution of the hydrolysable fraction of proteins and (C) of the hydrolysable carbohydrates to the POC in the three areas. Standard deviations of POC are reported. Vertical dotted lines: UML, oblique lines: deeper layer.

4.3. Hydrolysable proteins and carbohydrates of summer POM

Generally, the hydrolysable protein contribution was on average 35% of the total proteins during the ROME cruise. This was clearly lower than the contribution (higher than 90%) observed at coastal stations in the NW Mediterranean (Misic and Covazzi Harriague, 2008), and by Fabiano and Pusceddu (1998), who observed that 50% of the total proteins in TNB were hydrolysable. Besides the possibility that actual variations in time and space may occur, these differences may be due to the fact that the cited authors used trypsin to hydrolyse proteins, while in the present study, we used proteinase K. The hydrolysable carbohydrate contribution to total carbohydrates, instead, showed average values similar to those recorded in the previously cited NW Mediterranean (from 5 to 30%), but notably lower than the 80% found in TNB using the same method and hydrolytic enzyme. This pointed to sharp

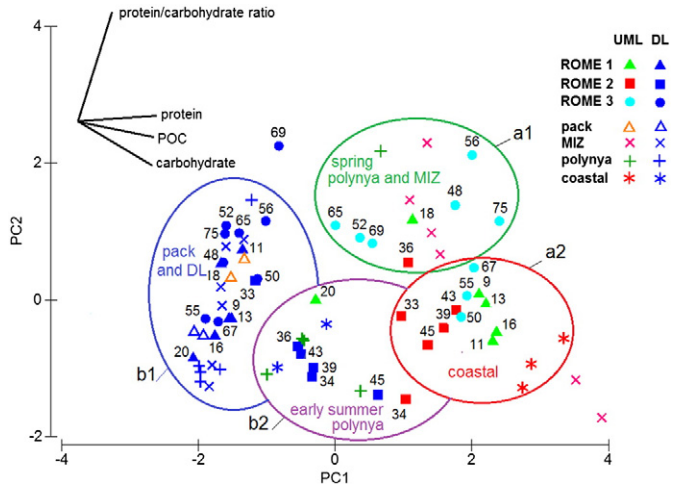

Fig. 6. PCA for the entire ROME cruise and the previous studies in the upper mixed layer (UML, coloured markers) and deeper layer (DL, blue markers). Two main groups (A and B) are composed of the sub-groups a1 and a2 (A), b1 and b2 (B). The ellipses are drawn following the results of the cluster analysis on the normalised data (Euclidean distance = 1.8). See text and Table 2 for details. The vectors of the variables are reported on the upper left of the plot.

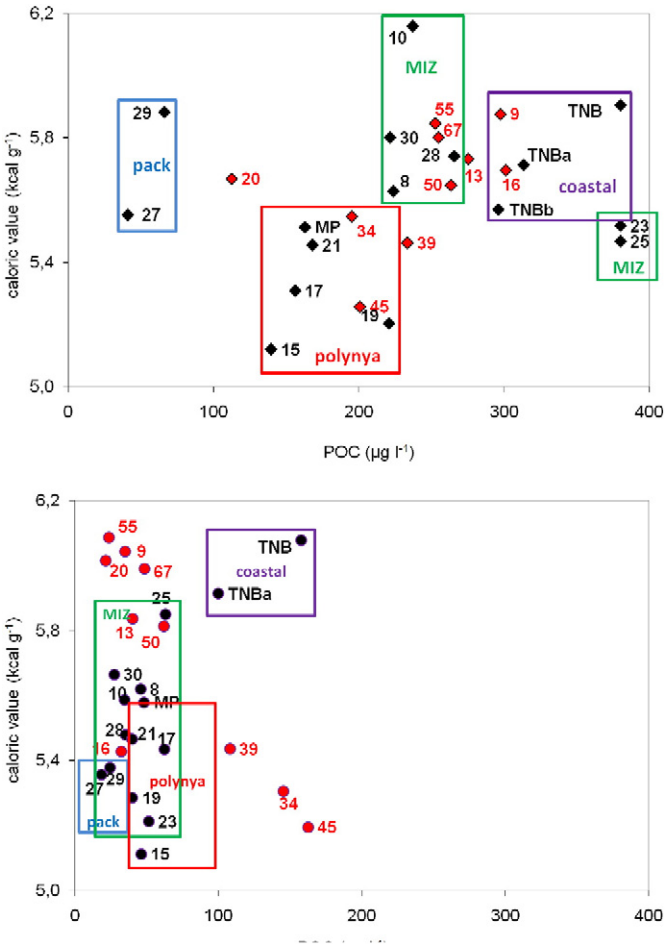

Fig. 7. Plot of the POC concentration and caloric value of the POM for the upper mixed layer (A) and the deeper layer (B). Black numbers and markers refer to the previous studies in the Ross Sea and coastal Terra Nova Bay (TNB) (see Table 2 for reference details), red numbers and markers refer to the ROME cruise results. Coloured boxes group the stations that have similar ice-related features (blue: pack-ice coverage, green: marginal ice zone – MIZ, red: polynya) or belong to the coastal sites (violet). See Table 2 for details.

spatial variations of the hydrolysable fraction of POM from the actual coastal area (Fabiano and Pusceddu, 1998) to the offshore area next to the polynya of TNB (this study). The vertical trends of the hydrolysable carbohydrates in the three ROME areas were different, reflecting a general influence by the environmental features on the distribution of the hydrolysable carbohydrate, but the relatively small size of our data set prevented deeper analysis of this item.

The main contribution to POC was given by the hydrolysable proteins, that showed slight, but interesting differences between the ROME areas and in the same area, following the mesoscale physical features.

Assuming that the POM production in the Ross Sea has a main phytoplankton signature (Fragoso and Smith, 2012), the fresh (generally more labile) POM should be found at the surface at the beginning of the productive season (spring), but the water vertical mixing of summer and the proliferation of the bacterial biomass would increase the quantity of labile heterotrophic materials such as proteins in the depth.

At the ROME sites the contribution of the labile proteinaceous C to the POC was, generally, higher in the deeper layer than in the mixed layer (Fig. 5A). In ROME 1 this proved true for the stations that had experienced longer ice-free conditions. Generally, in such areas, the relaxing of the stratification due to wind and waves allows a more homogeneous vertical distribution of POM by water-mass physical mixing. The lower maturity of station 20 (namely a higher ice-influence as revealed by salinity), instead, led to conditions more similar to spring, with a higher labile contribution at the surface.

ROME 2, instead, showed peculiar features. Despite being ice-free for the longest time and lying next to the winter polynya of TNB, its stations displayed a lower labile contribution in the deeper layer than in the UML. Station 39 was an exception, lying to the east of the hydrological

Table 4
Multivariate statistical analysis (ANOSIM and SIMPER) for the two main groups A and B of the PCA (Fig. 6) and the sub-groups a1-a2 and b1-b2. Mean values ± standard deviation for each group and sub-group are reported (particulate organic carbon (POC), proteins (PRT) and carbohydrates (CHO): $\mu g\ l^{-1}$; protein/carbohydrate ratio (PRT/CHO): $\mu g\ \mu g^{-1}$).

	ANOSIM		SIMPER					
Groups	R statistic	Significance	Variable	%		Average ± sd		Average ± sd
A vs B	0.847	0.1%	PRT	32	A:	281.4 ± 62.9	B:	58.8 ± 47.5
			PRT/CHO	25		3.6 ± 1.0		2.1 ± 0.9
			CHO	24		90.0 ± 32.9		32.7 ± 30.0
			POC	19		242.8 ± 55.0		72.4 ± 53.9
a1 vs a2	0.656	0.1%	PRT/CHO	41	a1:	4.3 ± 0.7	a2:	2.9 ± 0.4
			CHO	36		63.1 ± 15.7		115.1 ± 23.0
			PRT	14		243.8 ± 60.1		316.4 ± 43.0
b1 vs b2	0.903	0.1%	CHO	47	b1:	15.9 ± 5.5	b2:	71.5 ± 27.1
			PRT/CHO	22		2.2 ± 1.0		1.7 ± 0.4
			POC	17		40.7 ± 14.4		145.7 ± 36.6
			PRT	14		33.2 ± 17.1		118.0 ± 41.8

front and being influenced by an offshore current coming from the ROME 1 area. The other stations were separated from the actual offshore area by the front found at stations 34 and 45.

The vertical transport of the POM by vertical water mixing has a double relevance: it is essential for the foraging of bottom and mesopelagic communities, and it may contribute to the CO_2 biological pump. The occurrence of vertical transport, as shown by the ROME 2 and coastal observations in terms of bulk POM, may improve deep-sea nutrition, but also push C into the deep current system via the bottom-water. The vertical distribution of POM at the ROME 2 stations pointed to an efficient biological pump, because the POM accumulation was observed down to 200 m. The TNB area is characterised by the formation of dense water masses due to brine release during sea-ice production (HSSW) and by the freshening and cooling of the HSSW due to contact with the ice shelf (TISW). HSSW fills-up the deeper layer of the Drygalsky Basin and flows northwards until it reaches the shelf-break, which overflows down the continental slope, ventilating to the abyssal depths near Cape Adare (Jacobs et al., 1970; Whitworth and Orsi, 2006; Budillon et al., 2011). The deep layer POM of ROME 2 was more refractory, showing proportionally lower hydrolysable proteins and carbohydrates, higher POC/PON ratio, lower protein/carbohydrate ratio and a lower caloric content than the mixed layer. If refractivity is a limiting factor for the biological respiration of POM, it allows a more efficient burial of not respired C to the depth, indicating TNB as a sink for C in summer (Fonda Umani et al., 2002).

5. Conclusions

In this study, we firstly aimed at determining whether the POM was uniformly distributed in the Ross Sea area during a particular season (summer), when one of the main constraints regulating POM production and consumption (namely the ice cover) was generally lacking. We found that heterogeneity was still a dominant feature of the Ross Sea, due to the mesoscale characteristics of each area. The presence of fronts and eddies, with high current intensities, mixed the UML, stimulating phytoplankton production and POM accumulation. Nevertheless, the vertical and horizontal extent of this fertilisation was not continuous. The offshore ROME 1 and 3 areas differed from the ROME 2 area, especially with regard to the qualitative features of the POM. The deeper-layer POM was found to have higher lability in ROME 1 and 3, while the more coastal ROME 2 had the opposite trend. This may be relevant, because the POM of the deeper water, which would likely join the dense-water journey to the abyssal depths of the oceans, has a potentially lower trophic value and could be respired to a lesser extent, contributing to C storage in the bottom. On the other hand, enrichment of the deeper POM of the other areas via bacterial growth and high protein-containing phytoplankton would increase its trophic value, providing a valuable source of materials and energy for those consumers that also maintain metabolic activity during winter.

This study also highlighted that the heterogeneity of the offshore areas was principally a matter of the UML. This is a critical point, because the surface layer is the first to be influenced by climatic changes. Small atmospheric changes could lead to increased ecological changes, altering the fragile balance of the Southern Ocean.

Acknowledgements

We would like to thank the captain and crew of the R/V Italica for their unstinting assistance during the cruise. We are grateful to Paolo Povero and Enrico Olivari for their logistical support and for the hard sampling work, to Paola Rivaro, who provided the UML depths, and to Giorgio Budillon for the constructive discussion on the physical data. This study was conducted in the framework of the project “Ross Sea Mesoscale Experiment (ROME)” funded by the Italian National Program for Antarctic Research (PNRA, 2013/AN2.04).

Appendix A. Supplementary data

Supplementary data to this article can be found online at http://dx.doi.org/10.1016/j.jmarsys.2016.06.012.

References

Arrigo, K.R., van Djiken, G.L., 2004. Annual changes in sea-ice, chlorophyll a, and primary production in the Ross Sea, Antarctica. Deep-Sea Res. I 51, 117–138.
Arrigo, K.R., Worthen, D., Schnell, A., Lizotte, M.P., 1998. Primary production in Southern Ocean waters. J. Geophys. Res. 103, 15587–15600.
Arrigo, K.R., Lowry, K.E., vanDijken, G.L., 2012. Annual changes in sea ice and phytoplankton in polynyas of the Amundsen Sea, Antartica. Deep-Sea Res. II 5, 71–76.
Bligh, E.G., Dyer, W.J., 1959. A rapid method of total lipid extraction and purification. Can. J. Biochem. Physiol. 37, 911–917.
Budillon, G., Spezie, G., 2000. Thermohaline structure and variability in the Terra Nova Bay polynya, Ross Sea. Antarct. Sci. 12, 493–508.
Budillon, G., Pacciaroni, M., Cozzi, S., Rivaro, P., Catalano, G., Ianni, C., Cantoni, C., 2003. An optimum multiparameter mixing analysis of the shelf waters in the Ross Sea. Antarct. Sci. 15, 105–118.
Budillon, G., Castagno, P., Aliani, S., Spezie, G., Padman, L., 2011. Thermohaline variability and Antarctic bottom water formation at the Ross Sea shelf break. Deep-Sea Res. I 1002–1018.
Carlson, C.A., Ducklow, H.W., Hansell, D.A., Smith, W.O., 1998. Organic carbon partitioning during spring phytoplankton blooms in the Ross Sea polynya and the Sargasso Sea. Limnol. Oceanogr. 43 (3), 275–386.
Catalano, G., Povero, P., Fabiano, M., Benedetti, F., Goffart, A., 1997. Nutrient utilisation and particulate organic matter changes during summer in the upper mixed layer (Ross Sea, Antarctica). Deep-Sea Res. I 44, 97–112.
Celussi, M., Cataletto, B., Fonda Umani, S., Del Negro, P., 2009. Depth profiles of bacterioplankton assemblages and their activities in the Ross Sea. Deep-Sea Res. I 56, 2193–2205.
Comiso, J.C., McClain, C.R., Sullivan, C.W., Ryan, J.P., Leonard, C.L., 1993. Coastal zone color scanner pigment concentrations in the Southern Ocean and relationships to geophysical surface features. J. Geophys. Res. 98, 2419–2451.
Dall, W., Moriarty, D.J.W., 1983. Functional Aspects of Nutrition and Digestion. In: Mantel, L.H. (Ed.), The Biology of Crustacea Vol. 5. Academic Press, New York, pp. 215–261.
Davis, J., Benner, R., 2005. Seasonal trends in the abundance, composition and bioavailability of particulate and dissolved organic matter in the Chukchi/Beaufort seas and western Canada Basin. Deep-Sea Res. II 52, 3396–3410.
Dell'Anno, A., Fabiano, M., Mei, M.L., Danovaro, R., 2000. Enzymatically hydrolysed protein and carbohydrate pools in deep-sea sediments: estimates of the potentially bioavailable fraction and methodological considerations. Mar. Ecol. Prog. Ser. 196, 15–23.
Dubois, M., Gilles, K.A., Hamilton, J.K., Rebers, P.A., Smith, F., 1956. Colorimetric method for determination of sugars and related substances. Anal. Chem. 39, 350–356.
Dunbar, R.B., Leventer, A.R., Mucciarone, D.A., 1998. Water column sediment fluxes in the Ross Sea, Antarctica: atmospheric and sea ice forcing. J. Geophys. Res. 103 (30), 741–759.
Erofeeva, S.Y., Egbert, G.D., Padman, L., 2005. Assimilation of ship-mounted ADCP data for barotropic tides: application to the Ross Sea. J. Atmos. Ocean. Technol. 22, 721–734.
Etcheber, H., Relexans, J.-C., Beliard, M., Weber, O., Buscail, R., Heussner, S., 1999. Distribution and quality of sedimentary organic matter on the Aquitanian margin (Bay of Biscay). Deep-Sea Res. 46, 2249–2288.
Fabiano, M., Pusceddu, A., 1998. Total and hydrolizable particulate organic matter (carbohydrates, proteins and lipids) at a coastal station in Terra Nova Bay (Ross Sea, Antarctica). Polar Biol. 19, 125–132.
Fabiano, M., Povero, P., Danovaro, R., 1993. Distribution and composition of particulate organic matter in the Ross Sea (Antarctica). Polar Biol. 13, 525–533.
Fabiano, M., Danovaro, R., Crisafi, E., La Ferla, R., Povero, P., Acosta-Pomar, L., 1995. Particulate matter composition and bacterial distribution in Terra Nova Bay (Antarctica) during summer 1989-1990. Polar Biol. 15, 393–400.
Fabiano, M., Povero, P., Danovaro, R., 1996. Particulate organic matter composition in Terra Nova Bay (Ross Sea, Antarctica) during summer 1990. Antarct. Sci. 8, 7–13.
Fabiano, M., Chiantore, M., Povero, P., Cattaneo-Vietti, R., Pusceddu, A., Misic, C., Albertelli, G., 1997. Short-term variation in particulate matter flux in Terra Nova Bay, Ross Sea. Antarct. Sci. 9, 143–149.
Fabiano, M., Povero, P., Misic, C., 2000. Spatial and Temporal Distribution of Particulate Organic Matter in the Ross Sea. In: Faranda, F.M., Guglielmo, L., Ianora, A. (Eds.), Ross Sea Ecology. Springer, Berlin, pp. 135–150.
Fitch, D.T., Moore, J.K., 2007. Wind speed influence on phytoplankton bloom dynamics in the Southern Ocean marginal ice zone. J. Geophys. Res. 112, C08006. http://dx.doi.org/10.1029/2006JC004061.
Fonda Umani, S., Accornero, A., Budillon, G., Capello, M., Tucci, S., Cabrini, M., Del Negro, P., Monti, M., De Vittor, C., 2002. Particulate matter and plankton dynamics in the Ross Sea polynya of Terra Nova Bay during the austral summer 1997/1998. J. Mar. Syst. 36, 29–49.
Fragoso, G.M., Smith Jr., W.O., 2012. Influence of hydrography on phytoplankton distribution in the Amundsen and Ross seas, Antarctica. J. Mar. Syst. 89, 19–29.
Gardner, W.D., Richardson, M.J., Smith Jr., W.O., 2000. Seasonal patterns of water column particulate organic carbon and fluxes in the Ross Sea, Antarctica. Deep-Sea Res. II 47, 3423–3449.
Garrity, C., Ramseier, R.O., Peinert, R., Kern, S., Fischer, G., 2005. Water column particulate organic carbon modeled fluxes in the ice-frequented Southern Ocean. J. Mar. Syst. 56, 133–149.

Gordon Jr., D.C., 1970. Some studies on the distribution and composition of particulate organic carbon in the North Atlantic Ocean. Deep-Sea Res. 17, 233–243.
Hartree, E.F., 1972. Determination of proteins: a modification of the Lowry method that gives a linear photometric response. Anal. Biochem. 48, 422–427.
Hedges, J.I., Stern, J.H., 1984. Carbon and nitrogen determination of carbonate-containing solids. Limnol. Oceanogr. 29, 657–663.
Holm-Hansen, O., Lorenzen, C.J., Holmes, R.W., Strickland, J.D.H., 1965. Fluorometric determination of chlorophyll. J. Cons. int. Explor. Mer 30, 3–15.
Jacobs, S.S., Amos, A.F., Bruchhausen, P.M., 1970. Ross Sea oceanography and Antarctic bottom water formation. Deep-Sea Res. 17, 935–962.
Kim, B.K., Lee, J.H., Yun, M.S., Joo, H.T., Song, H.J., Yang, E.J., Chung, K.H., Kang, S.-H., Lee, S.H., 2014. High lipid composition of particulate organic matter in the northern Chukchi Sea, 2011. Deep-Sea Res. II 120, 72–81. http://dx.doi.org/10.1016/j.dsr2.2014.03.022i.
Kim, B.K., Lee, J.H., Joo, H.T., Song, H.J., Yang, E.J., Lee, S.H., Lee, S.H., 2016. Macromolecular compositions of phytoplankton in the Amundsen Sea, Antarctica. Deep-Sea Res. II 123, 42–49.
Kirchman, D.L., Meon, B., Ducklow, H.W., Carlson, C.A., Hansell, D.A., Steward, G.F., 2001. Glucose fluxes and concentrations of dissolved combined neutral sugars (polysaccharides) in the Ross Sea and polar front zone, Antarctica. Deep-Sea Res. II 48, 4179–4197.
Lee, S.H., Kim, B.K., Yun, M.S., Joo, H., Yang, E.J., Kim, Y.N., Shin, H.C., Lee, S., 2012. Spatial distribution of phytoplankton productivity in the Amundsen Sea, Antarctica. Polar Biol. 35, 1721–1733.
Mangoni, O., Modigh, M., Conversano, F., Carrada, G.C., Saggiomo, V., 2004. Effects of summer ice coverage on phytoplankton assemblages in the Ross Sea, Antarctica. Deep-Sea Res. I 51 (11), 1601–1617.
Marsh, J.B., Weinstein, D.B., 1966. A simple charring method for determination of lipids. J. Lipid Res. 7, 574–576.
Mayer, L.M., Schick, L.L., Sawyer, T., Plante, C.J., Jumars, P.A., Self, R.L., 1995. Bioavailable amino acids in sediments: a biomimetic, kinetics, based approach. Limnol. Oceanogr. 40, 511–520.
Misic, C., Covazzi Harriague, A., 2008. Organic matter recycling in a shallow coastal zone (NW Mediterranean): the influence of local and global climatic forcing and organic matter lability on hydrolytic enzyme activity. Cont. Shelf Res. 28, 2725–2735.
Misic, C., Povero, P., Fabiano, M., 2002. Ectoenzymatic ratios in relation to particulate organic matter distribution (Ross Sea, Antarctica). Microb. Ecol. 44, 224–234.
Monticelli, L.S., La Ferla, R., Maimone, G., 2003. Dynamics of bacterioplankton activities after a summer phytoplankton bloom period in Terra Nova Bay. Antarct. Sci. 15, 85–93.
Nelson, D.M., Demaster, D.J., Dunbar, R.B., Smith Jr., W.O., 1996. Cycling of organic carbon and biogenic silica in the Southern Ocean: estimates of water-column and sedimentary fluxes on the Ross Sea continental shelf. J. Geophys. Res. 10, 18519–18532.
Orsi, A.H., Wiederwohl, C.L., 2009. A recount of Ross Sea waters. Deep-Sea Res. II 56, 778–795. http://dx.doi.org/10.1016/ j.dsr2.2008.10.033.
Povero, P., Chiantore, M., Misic, C., Budillon, G., Cattaneo-Vietti, R., 2001. Land forcing controls pelagic-benthic coupling in Adélie cove (Terra Nova Bay, Ross Sea). Polar Biol. 24, 875–882.
Povero, P., Misic, C., Ossola, C., Castellano, M., Fabiano, M., 2003. The trophic role and ecological implications of oval faecal pellets in Terra Nova Bay (Ross Sea). Polar Biol. 26, 302–310.
Pusceddu, A., Dell'Anno, A., Fabiano, M., 2000. Organic matter composition in coastal sediments at Terra Nova Bay (Ross Sea) during summer 1995. Polar Biol. 23, 288–293.
Rigual-Hernández, A.S., Trull, T.W., Bray, S.G., Closset, I., Armand, L.K., 2015. Seasonal dynamics in diatom and particulate export fluxes to the deep sea in the Australian sector of the southern Antarctic zone. J. Mar. Syst. 142, 62–74.
Rivaro, P., Messa, R., Ianni, C., Magi, E., Budillon, G., 2014. Distribution of total alkalinity and pH in the Ross Sea (Antarctica) waters during austral summer 2008. Polar Res. 33, 20403. http://dx.doi.org/10.3402/polar.v33.20403.
Rivaro, P., Ianni, C., Langone, L., Ori, C., Aulicino, G., Cotroneo, Y., Saggiomo, M., Mangoni, O., 2017. Physical and biological forcing on the mesoscale variability of the carbonate system in the Ross Sea (Antarctica) during the summer season 2014. J. Mar. Syst. 166, 144–158.
Rossi, S., Isla, E., Martínez-García, A., Moraleda, N., Gili, J.-M., Rosell-Mele, A., Arntz, W.E., Gerdes, D., 2013. Transfer of seston lipids during a flagellate bloom from the surface to the benthic community in the Weddell Sea. Sci. Mar. 77, 397–407. http://dx.doi.org/10.3989/scimar.03835.30A.
Saggiomo, V., Carrada, G.C., Mangoni, O., Ribera d'Alcalà, M., Russo, A., 1998. Spatial and temporal variability of size-fractionated biomass and primary production in the Ross Sea (Antarctica) during austral spring and summer. J. Mar. Syst. 17, 115–127.
Saggiomo, V., Catalano, G., Mangoni, O., Budillon, G., Carrada, G.C., 2002. Primary production processes in ice-free waters of the Ross Sea (Antarctica) during the austral summer 1996. Deep-Sea Res. II 49, 1787–1801.
Sala, M.M., Arin, L., Balagué, V., Felipe, J., Guadayol, Ò., Vaqué, D., 2005. Functional diversity of bacterioplankton assemblages in western Antarctic seawaters during late spring. Mar. Ecol. Prog. Ser. 292, 13–21.
Schine, C.M.S., van Dijken, G., Arrigo, K.R., 2016. Spatial analysis of trends in primary production and relationship with large-scale climate variability in the Ross Sea, Antarctica (1997–2013). J. Geophys. Res. Oceans 121, 368–386. http://dx.doi.org/10.1002/2015JC011014.
Smith Jr., W.O., Asper, V.A., 2001. The influence of phytoplankton assemblage composition on biogeochemical characteristic and cycles in the Southern Ross Sea, Antarctica. Deep-Sea Res. I 48, 137–161.
Smith Jr., W.O., Nelson, D.M., Di Tullio, G.R., Leventer, A.R., 1996. Temporal and spatial patterns in the Ross Sea: phytoplankton biomass elemental composition, productivity and growth rates. J. Geophys. Res. 101, 18455–18466.
Smith Jr., W.O., Marra, J., Hiscock, M.R., Barber, R.T., 2000. The seasonal cycle of phytoplankton biomass and primary productivity in the Ross Sea, Antarctica. Deep-Sea Res. II 47, 3119–3140.
Smith Jr., W.O., Dinniman, M.S., Tozzi, S., DiTullio, G.R., Mangoni, O., Modigh, M., Saggiomo, V., 2010. Phytoplankton photosynthetic pigments in the Ross Sea: patterns and relationships among functional groups. J. Mar. Syst. 82, 177–185.
Soares, M.A., Bhaskar, P.V., Ravidas, R.K., Naik, K., Dessai, D., George, J., Tiwari, M., Anilkumar, N., 2015. Latitudinal $\delta^{13}C$ and $\delta^{15}N$ variations in particulate organic matter (POM) in surface waters from the Indian Ocean sector of Southern Ocean and the Tropical Indian Ocean in2012. Deep-Sea Res. II 118, 186–196.
Spreen, G., Kaleschke, L., Heygster, G., 2008. Sea ice remote sensing using AMSR-E 89 GHz channels. J. Geophys. Res. 113, C02S03. http://dx.doi.org/10.1029/2005JC003384.
Verdugo, P., Alldredge, A.L., Azam, F., Kirchman, D.L., Passow, U., Santschi, P.H., 2004. The oceanic gel phase: a bridge in the DOM–POM continuum. Mar. Chem. 92, 67–85.
Volkman, J.K., Tanoue, E., 2002. Chemical and biological studies of particulate organic matter in the ocean. J. Oceanogr. 58, 265–279.
Whitworth, T., Orsi, A.H., 2006. Antarctic bottom water production and export by tides in the Ross Sea. Geophys. Res. Lett. 33, L12609. http://dx.doi.org/10.1029/2006GL026357.
Winberg, G.G., 1971. Symbols, units and conversion factors in study of fresh waters productivity, Int. Biol. Programme Central Office, London, UK, pp. 1–25.
Young, J.N., Goldman, J.A.L., Kranz, S.A., Tortell, P.D., Morel, F.M.M., 2015. Slow carboxylation of Rubisco constrains the rate of carbon fixation during Antarctic phytoplankton blooms. New Phytol. 205, 172–181. http://dx.doi.org/10.1111/nph.13021.